

Probing Temperature Effects on the Hydrogen Bonding Network of the $\text{Cl}^-(\text{H}_2\text{O})_2$ Cluster

Helen E. Dorsett[†] and Robert O. Watts[‡]

Department of Chemistry, University of Melbourne, Parkville, VIC 3052, Australia

Sotiris S. Xantheas^{*}

Environmental Molecular Sciences Laboratory, Pacific Northwest National Laboratory, 906 Battelle Boulevard, P.O. Box 999, MS K1-96, Richland, Washington 99352

Received: October 28, 1998; In Final Form: March 19, 1999

We have incorporated the flexible RWK2 water potential into the parametrization of a chloride–water interaction potential from first principles calculations and used it to investigate the temperature effects in the infrared (IR) spectrum of $\text{Cl}^-(\text{H}_2\text{O})_2$. We have found that spectral signatures of hydrogen bonding between the two water molecules in the cluster disappear with increasing temperature, a consequence of the weak water–water interaction in the cluster.

I. Introduction

The study of aqueous ionic clusters provides molecular level information about interactions between the solvent and solute molecules. Of particular importance are the total and incremental association energies as well as the structures of the first few ion–water clusters as they constitute important benchmarks for the parametrization of interaction potentials used to study aqueous ionic solvation. Although thermodynamic quantities for the gas-phase hydration of several ions can be obtained solely from experimental measurements,¹ the elucidation of the structures of small aqueous clusters requires a combined experimental–theoretical effort.² The latter has relied primarily on the assignment of the measured vibrational spectra and their role as a “fingerprint” of the hydrogen bonding network of the cluster.

Previous first principles calculations^{3,4} suggested that chloride favors an “asymmetric” microhydration pattern in agreement with molecular dynamics simulations.⁵ Recently, the infrared spectra of small $\text{Cl}^-(\text{H}_2\text{O})_n$, $n < 5$ clusters have been measured⁶ in the 3000–4000 cm^{-1} region providing a direct probing of the network of OH stretches in the cluster.

In this study we present the parametrization of an interaction potential for chloride–water from first principles calculations. This potential is used to simulate the vibrational spectrum of the $\text{Cl}^-(\text{H}_2\text{O})_2$ cluster and probe the variation of its hydrogen bonding network as a function of temperature. We will, in particular, use the correspondence between structural and spectral trends in order to examine the temperature effect on the hydrogen bonding network of this cluster.

II. Interaction Potential

The energy of a cluster containing a chloride ion and n water molecules, V_n , is the sum of the intermolecular ion–water (V_{1k}^{inter}) and water–water (V_{ij}) pairwise additive interactions

and the intramolecular potential (V_k^{intra}) of the water molecule:

$$V_n = \sum_{k=1}^n (V_{1k}^{\text{inter}} + V_k^{\text{intra}}) + \sum_i^n \sum_{j<i}^n V_{ij} \quad (1)$$

where the index “1” denotes the ion and i, j, k are running indices over the water molecules.

The ion–water intermolecular interaction, V_{1k}^{inter} , is described by a combination of atom–atom and electrostatic terms between the ion ($q_{\text{Cl}} = -e$) and point charges placed within the water molecule according to the RWK2 convention,⁷ $q_{\text{H}} = +0.6e$ at each hydrogen and $Q = -2q_{\text{H}}$ centered at

$$\mathbf{R}_Q = \frac{d(\mathbf{R}_1 + \mathbf{R}_2)}{2R_0 \cos(\theta_0/2)} \quad (2)$$

where \mathbf{R}_1 and \mathbf{R}_2 are the position vectors of the hydrogen atoms with respect to the oxygen and $d = 0.26$ Å. The ion–water potential has the functional form

$$V_{1k}^{\text{inter}} = V_{\text{H-Cl}}(R) + V_{\text{O-Cl}}(R) + V_{\text{Q-Cl}}(R) \quad (3)$$

where

$$V_{\text{H-Cl}}(R) = A_{\text{H-Cl}} \exp(-\beta_{\text{H-Cl}} R) - \frac{q_{\text{H}}}{R} + L_{\text{H-Cl}}(R - R_{\text{H-Cl}}) + V_4(\beta_{\text{H-Cl}} R) \quad (4)$$

$$V_{\text{Q-Cl}}(R) = \frac{-Q}{R} + V_4(\beta_{\text{O-Cl}} R) \quad (5)$$

$$V_{\text{O-Cl}}(R) = A_{\text{O-Cl}} \exp(-\beta_{\text{O-Cl}} R) + V_4(\beta_{\text{O-Cl}} R) + V_6(\beta_{\text{O-Cl}} R) \quad (6)$$

and $L_{\text{H-Cl}}$ is a Morse oscillator function given by

$$L_{\text{H-Cl}}(r) = D_{\text{H-Cl}}((1 - e^{-\gamma_{\text{H-Cl}} r})^2 - 1) \quad (7)$$

* Author to whom correspondence should be addressed.

[†] Present address: Defense Science and Technology Organization, Salisbury, SA 5108, Australia.

[‡] Present address: BHP Research Laboratories, 245 Wellington Road, Mulgrave, VIC 3170, Australia.

TABLE 1: Ion–Water Intermolecular and Water–Water Intramolecular Potential Energy Parameters

Intermolecular Part			
$A_{HCl} = 9.0710 \text{ kcal mol}^{-1}$	$\beta_{HCl} = 0.55295 \text{ \AA}^{-1}$		
$A_{OCl} = 9067.3 \text{ kcal mol}^{-1}$	$\beta_{OCl} = 2.1386 \text{ \AA}^{-1}$		
$D_{HCl} = 2.5743 \text{ kcal mol}^{-1}$	$\gamma_{HCl} = 1.9795 \text{ \AA}^{-1}$	$R_{HCl} = 2.1308 \text{ \AA}$	
$\alpha_{Cl^-} = 3.69 \text{ \AA}^3$	$\alpha_{H_2O} = 1.47$		
$h\nu_{Cl^-} = 3.6127 \text{ eV}$	$h\nu_{H_2O} = 12.612 \text{ eV}$		
Intramolecular Part			
$D_1, D_2 = 131.25025 \text{ kcal mol}^{-1}$	$\gamma_1, \gamma_2 = 2.14125 \text{ \AA}^{-1}$	$R_0 = 0.9573 \text{ \AA}$	
$D_3 = 98.270 \text{ kcal mol}^{-1}$	$\gamma_3 = 0.70600 \text{ \AA}^{-1}$	$\theta_0 = 104.52^\circ$	
		$f_{12} = -15.1533 \text{ kcal mol}^{-1} \text{ \AA}^{-2}$	

The induction and dispersion terms, $V_{2n}(\beta R)$, have the form

$$V_{2n}(\beta R) = f_{2n}(\beta R) \frac{C_{2n}}{R^{2n}} \quad (8)$$

where $f_{2n}(\alpha R)$ is the “universal” damping function proposed by Tang and Toennies⁸

$$f_{2n}(\beta R) = 1 - \left(\sum_{k=0}^{2n} \frac{(\beta R)^k}{k!} \right) \exp(-\beta R) \quad (9)$$

The coefficients C_{2n} for long-range R^{-4} and R^{-6} interactions were estimated as:

$$C_4 = -\frac{1}{2} q_s^2 \alpha_t \quad (10)$$

$$C_6 = -\frac{3}{4} \left(\frac{h\nu_1 \times h\nu_2}{h\nu_1 + h\nu_2} \right) \alpha_1 \alpha_2 \quad (11)$$

where q_s and α_t are the ion charge and water polarizability and $h\nu_n$ and α_n are ionization potentials and polarizabilities of the interacting species.

Parameters for the ion–water interaction were determined by fitting to the MP4/aug-cc-pVTZ energies and coordinates along the $Cl^- \cdots O$ minimum-energy path.⁴ Small differences between the ab initio equilibrium water structure and the semiempirical model were resolved by fitting V_{lk}^{inter} to the magnitude of water distortion (i.e., ΔR_1 , ΔR_2 , and $\Delta \theta$) at fixed Cl–O separations. The parameters given in Table 1 yield a nearly exact fit to the ab-initio energies with fixed atomic coordinates. Analysis of energy gradients indicates that the model overestimates the Cl–H attraction for $R_{H-Cl} > 1.85 \text{ \AA}$. Nevertheless, the model reproduces the water orientation as a function of R_{O-Cl} almost exactly when compared to the ab-initio data. Allowing the model to relax at fixed Cl–O separations generates the energy profile given in Figure 1. The ab-initio data are also shown for comparison. The largest deviation between the two sets of data ($\chi^2 = 1.39$) occurs in the repulsive region of the potential.

The intramolecular water potential, V_k^{intra} , has the form:

$$V_k^{intra}(s_1, s_2, s_3) = \sum_{i=1}^3 M_i(s_i) + f_{12} s_1 s_2 \quad (12)$$

where $M_i(s_i)$ are Morse oscillator functions and s_i are local modes describing bend and stretch coordinates. The Morse parameters (D_i , α_i) and the coupling constant f_{12} were previously determined^{9,10} using a large basis set vibrational calculation to fit 56 vibrational levels for H_2O , D_2O , and HDO .

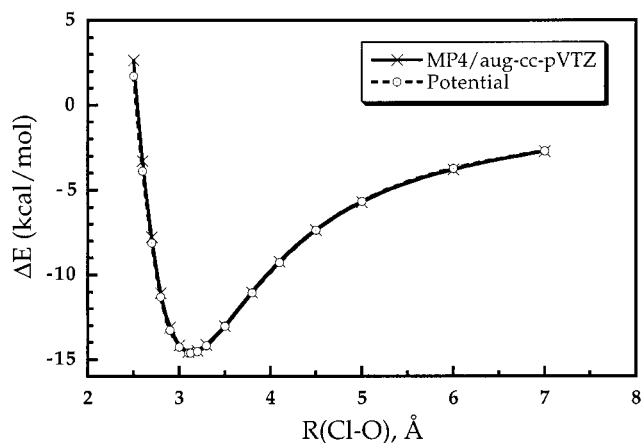


Figure 1. Minimum energy path (MEP) of chloride–water along the Cl–O distance. The ab-initio results (x) are from ref 4.

Finally for the water–water interaction, V_{ij} , we used the semiempirical RWK2 model, details of which are given elsewhere.⁷ This potential reproduces the water dipole and quadrupole moments, the second virial coefficient of steam, and several ice properties. It also has good values for the dispersion coefficients.

A 4-mode vibrational CI (VCI) calculation¹¹ with 3097 basis functions using our potential produces fundamentals of 3324 and 3764 cm^{-1} for the “hydrogen bonded” and “free” OH stretches of the $n = 1$ cluster, respectively. The potential overestimates the experimentally measured⁶ frequencies by 200 and 75 cm^{-1} respectively. It should be emphasized that the potential was parametrized using energetic and structural information only along the MEP for the approach of chloride to water. More accurate fundamental frequencies for the system can in principle be obtained using a larger and more representative grid of ab-initio points on the PES, a possibility that was not exploited in this study.¹²

III. Simulation of Infrared Spectra

We obtained temperature-dependent infrared spectra from the model potential by generating Boltzmann distributions of $Cl^-(H_2O)_2$ clusters with the Metropolis Monte Carlo method¹³ and then performing a “frozen-field” local-mode vibrational analysis¹⁴ on the resulting configurations. This approach defines a “reference configuration” by assuming that every intramolecular mode of water in the cluster behaves as an independent Morse oscillator. The cluster is distorted from its original configuration along each local mode (s_1, s_2, s_3) holding all other variables fixed. A Morse potential function is fitted to the potential energy calculated along every coordinate, and the eigenfunctions of these effective potentials are used to generate a mean field basis set. Eigenvalues are estimated using third-order variational calculations to include off-diagonal kinetic and potential energy couplings. Band intensities are calculated by including changes in both the permanent and induced dipole moments of the water molecules in the cluster when calculating transition moments. That is, the stretching vibration of an O–H bond near the highly polarizable chloride ion produces a larger change in the induced dipole—and thus is more intense. At a site i with polarizability α_i in the cluster, the induced dipole moment is given by

$$\mu_i = \alpha_i E_i \quad (13)$$

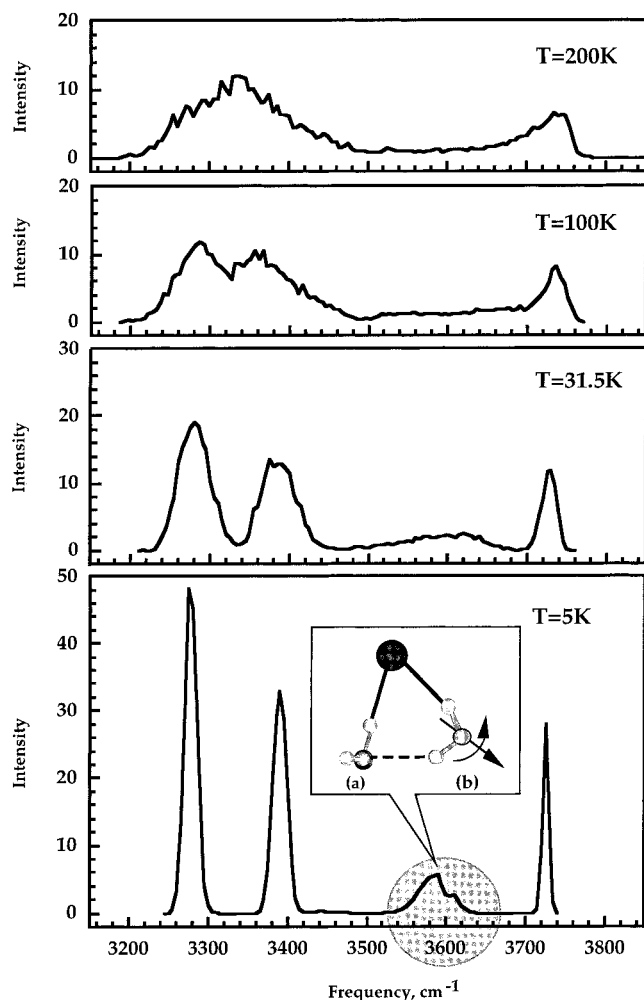


Figure 2. Computed vibrational spectra for $\text{Cl}^-(\text{H}_2\text{O})_2$ at $T = 5, 31.5, 100,$ and 200 K. The peak at ~ 3580 cm^{-1} arises from hydrogen bonding between the two water molecules which is lost at high temperatures.

where

$$E_i = \sum_{j \neq i} \frac{q_j \mathbf{r}_{ij}}{r_{ij}^3} + \sum_{j \neq i} \frac{1}{r_{ij}^3} \left(\frac{3\mathbf{r}_{ij} \mathbf{r}_{ij}}{r_{ij}^2} - 1 \right) \boldsymbol{\mu}_j \quad (14)$$

Hence, for each local mode displacement, an iterative procedure is used to solve eqs 13 and 14. Convergence is achieved when deviations of the dipole moment from two sequential iterations fall within 0.001 D/atom. We use the charges and polarizabilities of the ion–water model, but assume that point charges and polarizabilities within a water molecule do not interact with each other, and that intramolecular vibrations do not affect the water polarizability.

IV. Results and Discussion

The optimum geometry of the $\text{Cl}^-(\text{H}_2\text{O})_2$ cluster, shown in the insert of Figure 2, exhibits a “cyclic” structure with two “ionic” hydrogen bonds (solid lines; represent water molecules bonded to chloride) and a hydrogen bond between the two water molecules (dashed line). As noted earlier,⁴ the hydrogen bond between the two water molecules is weak (the two-body attractive water–water interaction is just -1.21 kcal/mol). This fact can, for instance, facilitate rotation of one of the water molecules around the Cl–O axis as shown in Figure 2 with a simultaneous breaking of the water–water hydrogen bond. Isomerization of the cluster along this direction proceeds via a

first-order transition state of C_2 symmetry having an imaginary frequency of 140 cm^{-1} and an electronic energy barrier of 0.52 kcal/mol (0.17 kcal/mol with inclusion of zero-point energies) at the MP2/aug-cc-pVDZ level of theory. This isomerization pathway is lower in energy than the one proceeding via a C_{2h} transition state⁴ of higher order (3 imaginary frequencies) which lies 2.2 kcal/mol above the minimum. Although our current model does not utilize a polarizable potential for water it seems to reproduce the energy difference between the minimum and the C_2 transition state quite well (0.56 kcal/mol) when compared to the ab-initio result (0.52 kcal/mol). The (three-body) ion–water–water interaction was previously reported⁴ to be quite small for the minimum configuration of the $n = 2$ cluster ($+0.7$ kcal/mol); it is presumably of comparable magnitude at the C_2 transition state, a fact justifying the reproduction of the magnitude of this barrier with an “effective two-body” model such as the one used in this study.

The calculated spectra at four different temperatures ($5, 31.5, 100,$ and 200 K) in the 3100 – 3900 cm^{-1} region are shown in Figure 2. The “cold” spectra ($T = 5$ and 31.5 K) exhibit four distinct peaks at $3275, 3390, 3590,$ and 3725 cm^{-1} corresponding to the two ionic bonds (OH stretches hydrogen bonded to chloride), the water–water hydrogen bond and the “free” OH stretch, respectively. This spectral pattern is consistent with the “ $T = 0$ K” picture reported earlier⁴ from ab-initio calculations as well as recent experimental measurements. The experimentally observed peaks are at $3130, 3375, 3633,$ and 3686 cm^{-1} , respectively.¹⁵ At higher temperatures, however, the peak at ~ 3600 cm^{-1} associated with the water–water interaction disappears. This is consistent with the expectation that at elevated temperatures there will be significant sampling of both the C_2 and intermediate configurations exhibiting no hydrogen bonding between the water molecules. For instance, the Boltzmann factor for the probability of accessing the C_2 configuration (assuming $\Delta E = 0.17$ kcal/mol) is 0.3 at 100 K and 0.4 at 200 K. Another striking difference at the higher temperatures ($T = 100$ K) is that the two “ionic” peaks tend to merge together. As previously⁴ discussed, the minimum energy geometry of the $n = 2$ cluster can be built starting from the $n = 1$ cluster [chloride and water (a) in Figure 2] with the second water molecule (b) trying to maximize the hydrogen bonding with the remaining system. This results in two “ionic” bonds that have unequal Cl–O bond lengths and strengths. At higher temperatures due to the breaking of the water–water hydrogen bond the reason for discriminating between the two ionic bonds is removed and so does its signature in the IR spectra. The breaking of the inter-water hydrogen bond has been previously experimentally observed¹⁶ for the $\text{I}^-(\text{H}_2\text{O})_2$ system.

A measure of the sampling of the configuration space away from the minimum at different temperatures is provided by the pair distribution functions¹⁷ $g_{\text{O}\cdots\text{H}}(r)$ and $g_{\text{O}\cdots\text{O}}(r)$. These are the probabilities of finding atom “A” at distance r from atom “B” and are shown in Figures 3 and 4. The peak at ~ 2 Å for $g_{\text{O}\cdots\text{H}}(r)$ (Figure 4) corresponds to the hydrogen bonded O⋯H pair between the two water molecules. At high temperatures this peak broadens and eventually disappears along with the hydrogen bond between the two water molecules. The same pattern is observed for the O–O pair distribution function (Figure 4). At low temperatures the distribution is quite narrow (fwhm ~ 0.1 Å), and it broadens at higher temperatures as a result of sampling configurations with larger O–Cl–O angles. This result is consistent with similar trends in the pair distribution functions previously observed¹⁸ for the $\text{Cl}^-(\text{H}_2\text{O})_n$ and $\text{I}^-(\text{H}_2\text{O})_n$ clusters using rigid water potentials. However, rigid

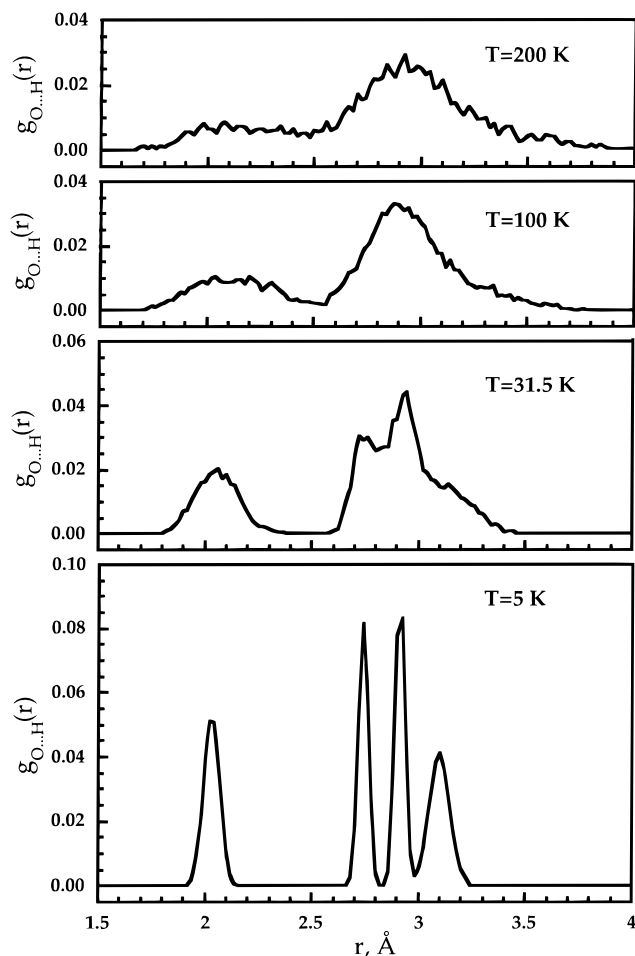


Figure 3. Pair distribution function $g_{O...H}(r)$ for $\text{Cl}^-(\text{H}_2\text{O})_2$ at $T = 5, 31.5, 100,$ and 200 K.

water potentials cannot address issues related to the intramolecular motion examined in this study. During these previous studies a comparison was made between the classical and quantum mechanical treatments of nuclear motion.¹⁹ We plan to revisit these issues in the future for this and larger chloride-water clusters with a polarizable extension of the present potential that includes intramolecular degrees of freedom.

Conclusions

Due to the weak water-water interaction in $\text{Cl}^-(\text{H}_2\text{O})_2$, temperature has dramatic effects in altering the hydrogen bonding network between the two water molecules and its signature in the IR spectra. "Cold" spectra exhibit characteristics of hydrogen bonding between the two water molecules whereas these features are weakening and finally disappearing with increasing temperature.

Acknowledgment. We thank M. Okumura, M. Johnson, and G. Schenter for useful discussions; J. Bowman for providing the VCI results for $\text{Cl}^-(\text{H}_2\text{O})$; and B. Gerber for providing a preprint of his work. Dr. Jeff Reimers is thanked for valuable discussions and for supplying the basic computer codes used to simulate the vibrational spectra. Part of this work was performed under the auspices of the Division of Chemical Sciences, Office of Basic Energy Sciences, U.S. Department of Energy under Contract DE-AC06-76RLO 1830 with Battelle Memorial Institute, which operates the Pacific Northwest National Laboratory. We also acknowledge support from the Australian Research Council. H.E.D. acknowledges an Associ-

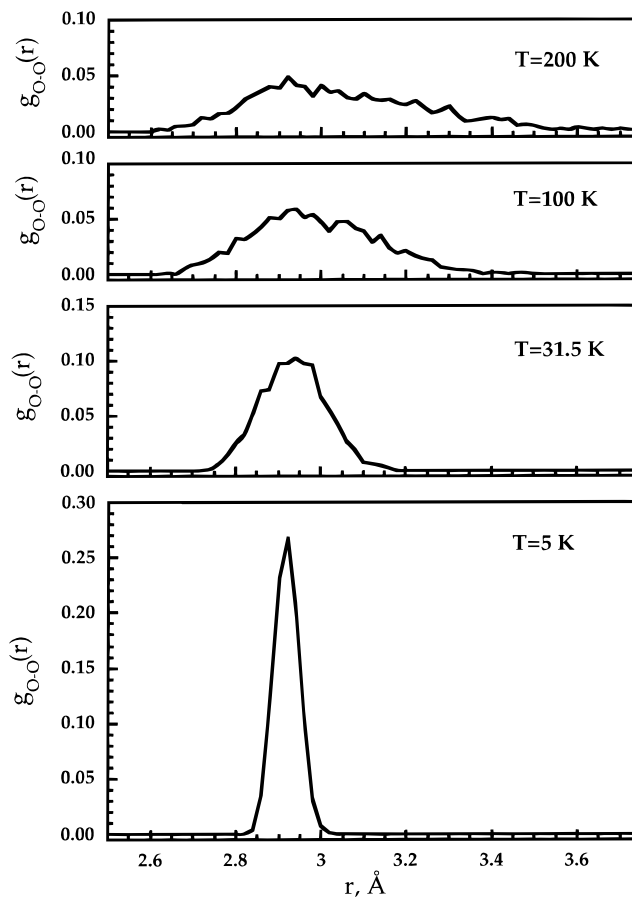


Figure 4. Pair distribution function $g_{O-O}(r)$ for $\text{Cl}^-(\text{H}_2\text{O})_2$ at $T = 5, 31.5, 100,$ and 200 K.

ated Western Universities Fellowship during a visit to PNNL from November 1, 1997 to January 31, 1998. Computer resources were provided by the Division of Chemical Sciences and by the Scientific Computing Staff, Office of Energy Research, at the National Energy Research Supercomputer Center (Berkeley, CA).

References and Notes

- (1) Arshadi, M.; Yamdagni, R.; Kebarle, M.; *J. Phys. Chem.* **1970**, *74*, 1475; Arshadi, M.; Kebarle, P. *J. Phys. Chem.* **1970**, *74*, 1483. For recent reviews, see Keese, R. G.; Castleman, A. W., Jr. *J. Phys. Chem. Ref. Data* **1986**, *15*, 1011 and Ohtaki, H.; Radnai, T. *Chem. Rev.* **1993**, *93*, 1157.
- (2) Pribble, R. N.; Zwier, T. S. *Science* **1994**, *265*, 75; Liu, K.; Cruzan, J. D.; Saykally, R. J. *Science* **1996**, *271*, 929; Liu, K.; Brown, M. G.; Carter, C.; Saykally, R. J.; Gregory, J. K.; Clary, D. C. *Nature* **1996**, *381*, 501; Gruenloh, C. J.; Carney, J. R.; Arrington, C. A.; Zwier, T. S.; Fredericks, S. Y.; Jordan, K. D. *Science* **1997**, *276*, 1678; Buck, U.; Ettischer, I.; Melzer, M.; Buch, V.; Sadlej, J. *Phys. Rev. Lett.* **1998**, *80*, 2578; Cabarcos, O. M.; Weinheimer, C. J.; Lisy, J. M.; Xantheas, S. S. *J. Chem. Phys.* **1999**, *110*, 5.
- (3) Combariza, J. E.; Kestner, N. R.; Jortner, J. *Chem. Phys. Lett.* **1993**, *203*, 423; Combariza, J. E.; Kestner, N. R.; Jortner, J. *J. Chem. Phys.* **1994**, *100*, 2851; Combariza, J. E.; Kestner, N. R. *J. Phys. Chem.* **1995**, *99*, 2717.
- (4) Xantheas, S. S. *J. Phys. Chem.* **1996**, *100*, 9703.
- (5) Dang, L. X.; Smith, D. E. *J. Chem. Phys.* **1993**, *99*, 6950; Perera, L.; Berkowitz, M. L. **1994**, *100*, 3085.
- (6) Choi, J.-H.; Kuwata, K. T.; Cao, Y.-B.; Okumura, M. *J. Phys. Chem.* **1998**, *102*, 503; Ayotte, P.; Weddle, G. H.; Kim, J.; Johnson, M. A. *J. Am. Chem. Soc.* **1998**, *120*, 12361; Ayotte, P.; Bailey, C. G.; Weddle, G. H.; Johnson, M. A. *J. Phys. Chem. A* **1998**, *102*, 3067.
- (7) Reimers, J. R.; Watts, R. O.; Klein, M. L. *Chem. Phys.* **1982**, *64*, 95.
- (8) Tang, K. T.; Toennies, J. P. *J. Chem. Phys.* **1984**, *80*, 3726.
- (9) Reimers, J. R.; Watts, R. O. *Mol. Phys.* **1984**, *52*, 357.
- (10) Coker, D. F.; Miller, R. E.; Watts, R. O. *J. Chem. Phys.* **1985**, *82*, 3554.

- (11) Carter, S.; Bowman, J. M.; Harding, L. B. *Spectrochim. Acta A* **1997**, 53, 1179; Carter, S.; Culik, S.; Bowman, J. M. *J. Chem. Phys.* **1997**, 107, 10458; Carter, S.; Bowman, J. M. *J. Chem. Phys.* **1998**, 108, 4397; Carter, S.; Bowman, J. M. and Handy, N. C. *Theor. Chem. Acc.*, in press.
- (12) Chaban, G. M.; Jung, J. O.; Gerber, R. B. Preprint.
- (13) Metropolis, N.; Rosenbluth, A. W.; Rosenbluth, M. N.; Teller, A. H.; Keller, E. J. *J. Chem. Phys.* **1953**, 6, 1087.
- (14) Reimers, J. R.; Watts, R. O. *Chem. Phys.* **1984**, 85, 83.
- (15) Ayotte, P.; Johnson, M. A. Unpublished work.
- (16) Ayotte, P.; Weddle, G. H.; Kim, J.; Johnson, M. A. *Chem. Phys.* **1998**, 239, 253.
- (17) Allen, M. P.; Tildsley, D. J. *Computer Simulation of Liquids*; Oxford University Press: New York, 1987.
- (18) Garrett, B. C.; Schenter, G. K.; Gai, H.; Dang, L. X. In *Advances in Classical Trajectory Methods*, Vol. 3; Hase, W. L., Ed.; JAI Press: Stamford, CT 1998, pp 1–33.
- (19) Gai, H.; Dang, L. X.; Schenter, G. K.; Garrett, B. C. *J. Phys. Chem.* **1995**, 99, 13303.